Figure S1

A

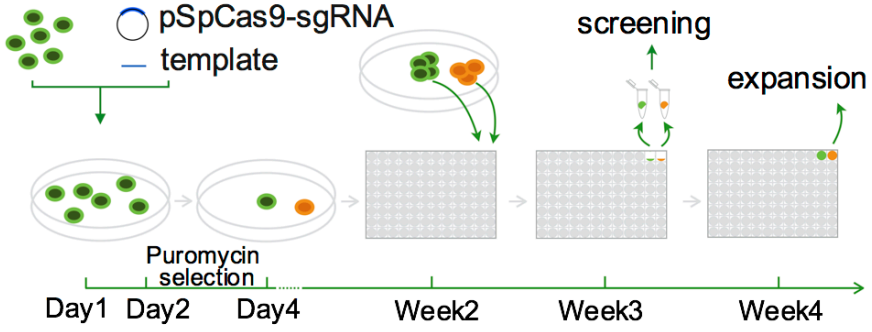

C

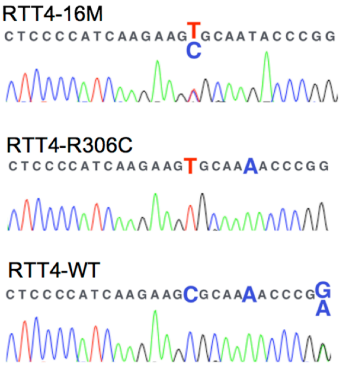

B

Target: 5'-CTCCCCATCAAGAAGCGCAAGACCCGGGAG-3'

SmaI

Template: 5'-...CTCCCCATCAAGAAGTGCAAAACCCGAGAG...-3' (102 bp)

C916T

		sgRNA targeting		HDR	
		Colony number	Efficiency	Colony number	Efficiency
Total targeting		28/70	40.0%		
Number of Alleles Targeted	1	14/70	20.0%		
	2	14/70	20.0%		
HDR				2/70	2.9%

D

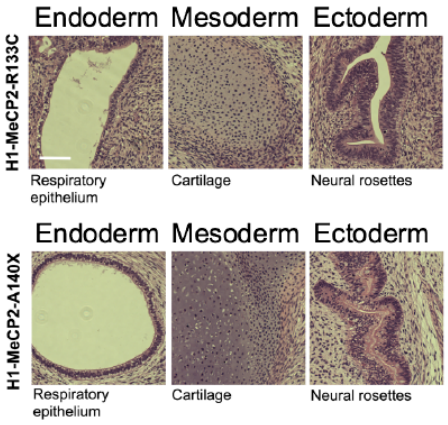

E

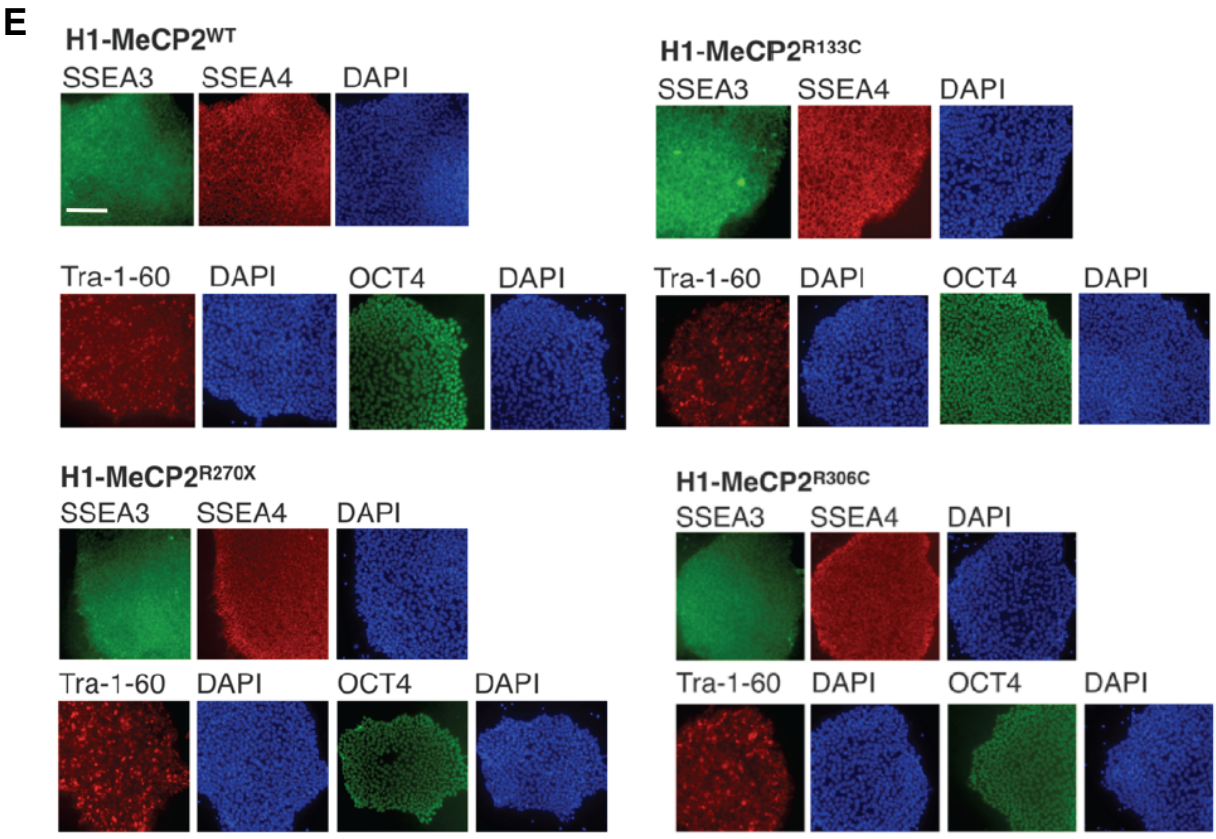

Figure S1. Related with Figure 1. CRISPR/Cas9-mediated MeCP2 Editing and Characterization of Edited hESCs

(A) Schematic view of protocol for CRISPR/Cas9-mediated genome editing in hPSCs. Details are described in methods.

(B) Design of CRISPR/Cas9-mediated MECP2 editing in hiPSC line RTT4-16M. Red color indicates desired mutations introduced, blue color indicates synonymous changes, and green color indicates PAM sequence.

(C) Sequences of targeted locus in edited RTT4-16M clones.

(D) In vivo formation of three germ layers of randomly selected MeCP2 mutant hESCs. The scale bar represents 50 μm.

(E) Expressions of pluripotent markers in MeCP2-WT and MeCP2-mutant hESCs. The scale bar represents 50 μm.

Figure S2

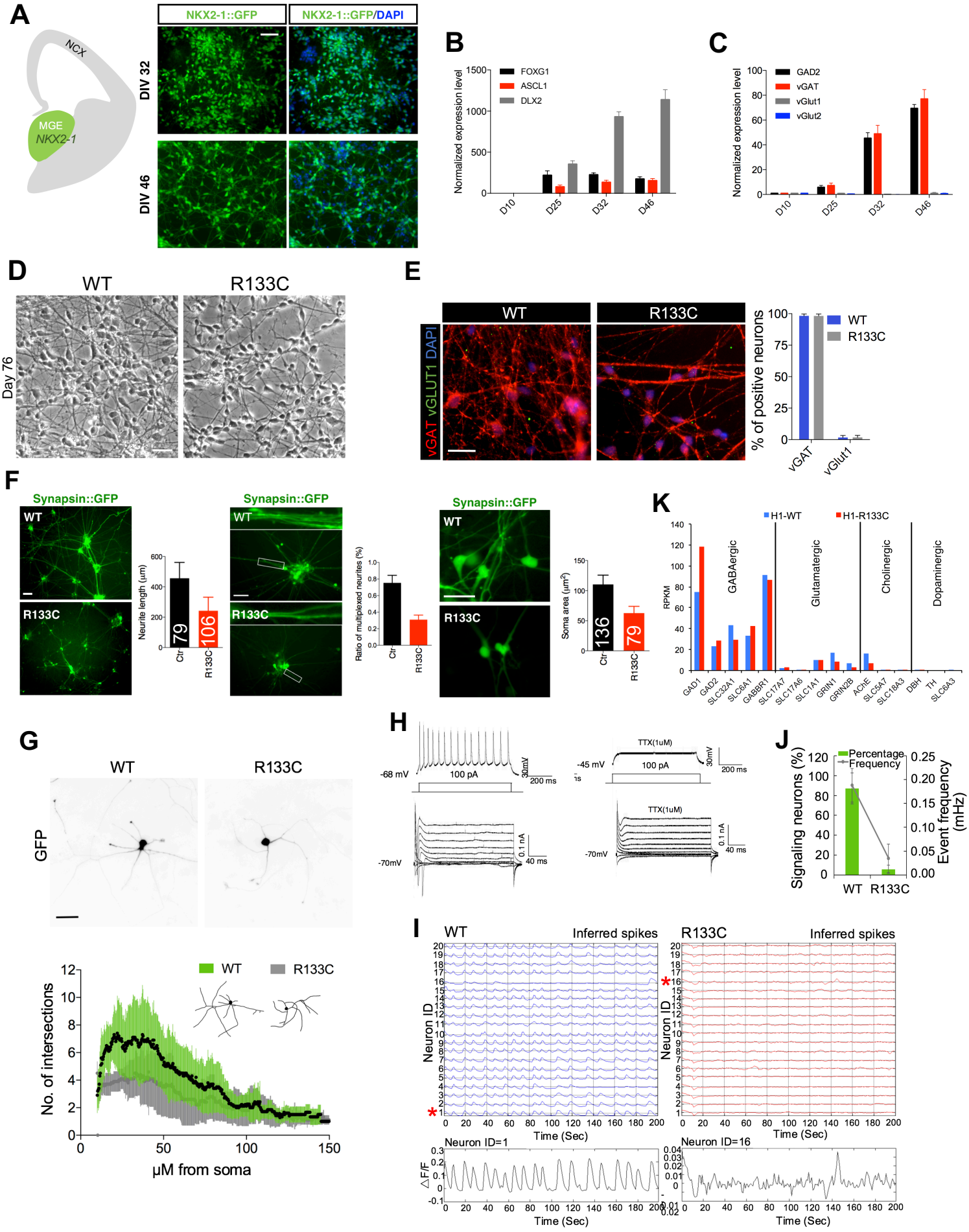
A
NCX
MGE
NKX2-1
NKX2-1::GFP
NKX2-1::GFP/DAPI
DIV 32
DIV 46
B
Normalized expression level
FOXG1
ASCL1
DLX2
D10
D25
D32
D46
C
Normalized expression level
GAD2
vGAT
vGlut1
vGlut2
D10
D25
D32
D46
D
WT
R133C
Day 76
E
WT
R133C
vGAT vGLUT1 DAPI
% of positive neurons
WT
R133C
vGAT
vGlut1
F
Synapsin::GFP
WT
R133C
Neurite length (μm)
79
106
Ctr
R133C
Ratio of multiplexed neurites (%)
Soma area (μm²)
136
79
K
H1-WT
H1-R133C
RPKM
GABAergic
Glutamatergic
Cholinergic
Dopaminergic
GAD1
GAD2
SLC32A1
SLC6A1
GABBR1
SLC17A7
SLC17A6
SLC1A1
GRIN1
GRIN2B
AChE
SLC5A7
SLC18A3
DBH
TH
SLC6A3
G
WT
R133C
GFP
No. of intersections
μM from soma
H
-68 mV
100 pA
30mV
200 ms
-70mV
0.1 nA
40 ms
-45 mV
TTX(1uM)
J
Signaling neurons (%)
Percentage
Frequency
Event frequency (mHz)
WT
R133C
I
WT
R133C
Inferred spikes
Neuron ID
Time (Sec)
Neuron ID=1
Neuron ID=16
ΔF/F

Figure S2. Related with Figure 1. Characterization of Directly Differentiated Human INs
(A) The major region for IN production (left) and the generation of high-purity NKX2-1$^+$ MGE progenitors using the IN differentiation protocol (right). Note NKX2-1$^+$ MGE is the ventral part of forebrain where INs are produced, and with the applied differentiation protocol, homogeneous NKX2-1-GFP$^+$ progenitors were produced. The scale bar represents 50 μm.
(B and C) Expressions of markers for IN development as detected by qPCR. Mean ± SD is shown (n=3 technical repeats of the same batch of RNA pellets).
(D) Phase-contrast micrographs of MeCP2-WT and MeCP2-R133C INs at day 76. The scale bar represents 20 μm.
(E) Immunostaining and quantification of vGAT and vGLUT1 in MeCP2-WT and MeCP2-R133C INs. Mean ± SD is shown for each condition (n=3 biologically independent samples).
(F) MeCP2-R133C INs showed deceased neurite length (left) (n=79 and 106 neurites of neurons from 3 independently treated wells for MeCP2-WT and MeCP2-R133C INs, respectively), neurite interaction (middle) (n=5 independently treated wells), and soma size (right) (n=136 and 79 cells from 5 independently treated wells for MeCP2-WT and MeCP2-R133C INs, respectively). Mean ± SD is shown. Neurite and cell numbers used for quantification are labeled. INs were transduced with AAV1.hSyn.eGFP vectors at 9 weeks of maturation (day 81) and the above assays were performed at 12 weeks of maturation (day 102). Images from live IN cultures were acquired and used for quantification. The scale bar represents 25 μm.
(G) Representative images of MeCP2-WT and MeCP2-R133C IN morphologies and Sholl analysis of dendrite complexity. INs were transduced with AAV1.hSyn.eGFP vectors at day 67 and sparsely re-plated on to mouse astrocytes on day 77. Samples were fixed and stained with anti-GFP antibody after additional 4 days' culturing. Images were randomly acquired and individually positioned MeCP2-WT (n=10 neurons from 2 independent wells) or MeCP2-R133C (n=10 neurons from 2 independent wells) INs without dendritic intersection with neighboring neurons were used for quantification. The scale bar represents 20 μm.
(H) Representative images of action potential, sodium and potassium currents in MeCP2-WT INs before and after TTX treatment at 8 weeks of maturation (day 74).
(I) Calcium spikes of MeCP2-WT and MeCP2-R133C INs. INs were transduced with AAV1.syn.GCaMP6s.WPRE.SV40 vectors at 7 weeks of maturation (day 67) and calcium imaging was performed at 11 weeks of maturation (day 98). Spiking pattern of representative INs labeled by red stars are enlarged on the bottom.
(J) Quantification of percentage of signaling neurons (n=4 independently treated wells) and frequency of calcium surges (n=47 signaling MeCP2-WT neurons from 4 independently treated wells, and n=4 signaling MeCP2-R133C neurons from 4 independently treated wells). Mean ± SD is shown.
(K) Expressions of markers for various neuronal types in day 74 MeCP2-WT and MeCP2-R133C INs detected by RNA-seq.

Figure S3

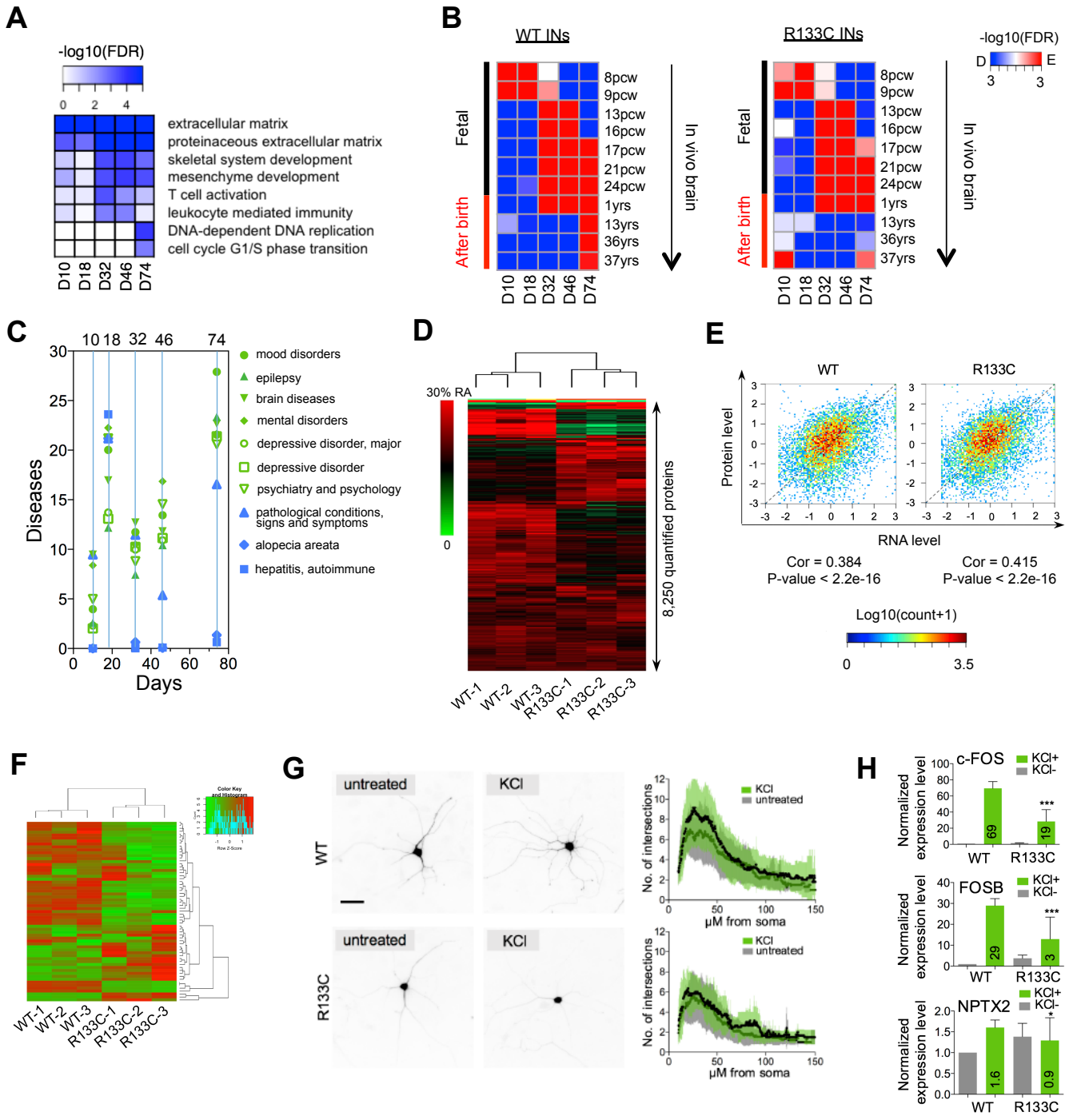
A
-log10(FDR)
0 2 4
extracellular matrix
proteinaceous extracellular matrix
skeletal system development
mesenchyme development
T cell activation
leukocyte mediated immunity
DNA-dependent DNA replication
cell cycle G1/S phase transition
D10 D18 D32 D46 D74
B
WT INs
R133C INs
-log10(FDR)
D E
3 3
Fetal
After birth
In vivo brain
8pcw
9pcw
13pcw
16pcw
17pcw
21pcw
24pcw
1yrs
13yrs
36yrs
37yrs
D10 D18 D32 D46 D74
C
10 18 32 46 74
Diseases
Days
mood disorders
epilepsy
brain diseases
mental disorders
depressive disorder, major
depressive disorder
psychiatry and psychology
pathological conditions, signs and symptoms
alopecia areata
hepatitis, autoimmune
D
30% RA
0
8,250 quantified proteins
WT-1 WT-2 WT-3 R133C-1 R133C-2 R133C-3
E
WT
R133C
Protein level
RNA level
Cor = 0.384
P-value < 2.2e-16
Cor = 0.415
P-value < 2.2e-16
Log10(count+1)
0 3.5
F
WT-1 WT-2 WT-3 R133C-1 R133C-2 R133C-3
G
untreated
KCl
WT
R133C
No. of intersections
μM from soma
KCl
untreated
H
c-FOS
FOSB
NPTX2
KCl+
KCl-
Normalized expression level
69
19
29
3
1.6
0.6
***
*
WT
R133C

Figure S3. Related with Figure 1. Transcriptome and Proteome Analysis of Human INs
(A) GOs of genes down-regulated during MeCP2-WT IN development. Genes related to DNA replication and cell cycle transition were down-regulated in mature INs (day 74).
(B) GSEA of gene signatures for *in vivo* human brain development. Enrichment and depletion of the gene signature (-log10(FDR)) in INs at each time point are shown by red and blue color, respectively.
(C) Disease analysis based on differential expressions of biomarkers between MeCP2-WT and MeCP2-R133C samples.
(D) Heat map of proteomic profiling in day 76 MeCP2-WT and MeCP2-R133C INs. 3 biologically independent samples for both MeCP2-WT and MeCP2-R133C INs were profiled.
(E) Comparative analysis of RNA (day 74) and protein (day 76) levels in mature MeCP2-WT and MeCP2-R133C INs. Z score for log2-transformed RPKM and intensity are plotted in X and Y axis, respectively. Pearson correlation coefficient and its p-value are shown.
(F) Heat map of protein levels of calcium-related cellular components in day 76 MeCP2-WT and MeCP2-R133C INs. 3 biologically independent samples for both MeCP2-WT and MeCP2-R133C INs are shown.
(G) Dendrite complexity of INs before and after KCl depolarization and the corresponding Sholl analysis. INs were transduced with AAV1.hSyn.eGFP vectors at day 67 and sparsely re-plated on to mouse astrocytes on day 77. 2 days after plating, KCl buffer (final concentration: 25 mM) was supplemented to the media, and samples were fixed and stained with anti-GFP antibody after additional 2 days' culturing. Images were randomly acquired and individually positioned MeCP2-WT (n=12 neurons from 2 independent wells), MeCP2-WT+KCl (n=12 neurons from 2 independent wells), MeCP2-R133C (n=6 neurons from 2 independent wells), or MeCP2-R133C+KCl (n=13 neurons from 2 independent wells) INs without dendritic intersection with neighboring neurons were used for quantification. The scale bar represents 20 μm.
(H) Depolarization-induced expressions of IEGs c-FOS, FOSB, and NPTX2 in day 74 INs. Fold numbers relative to non-KCl groups are labeled. Mean ± SD is shown (n=3 technical repeats of the same batch of RNA pellets). KCl-induced fold changes were compared between MeCP2-WT and MeCP2-R133C groups for statistical significance. ***$p < 0.001$, *$p < 0.05$ (unpaired t-test).

Figure S4

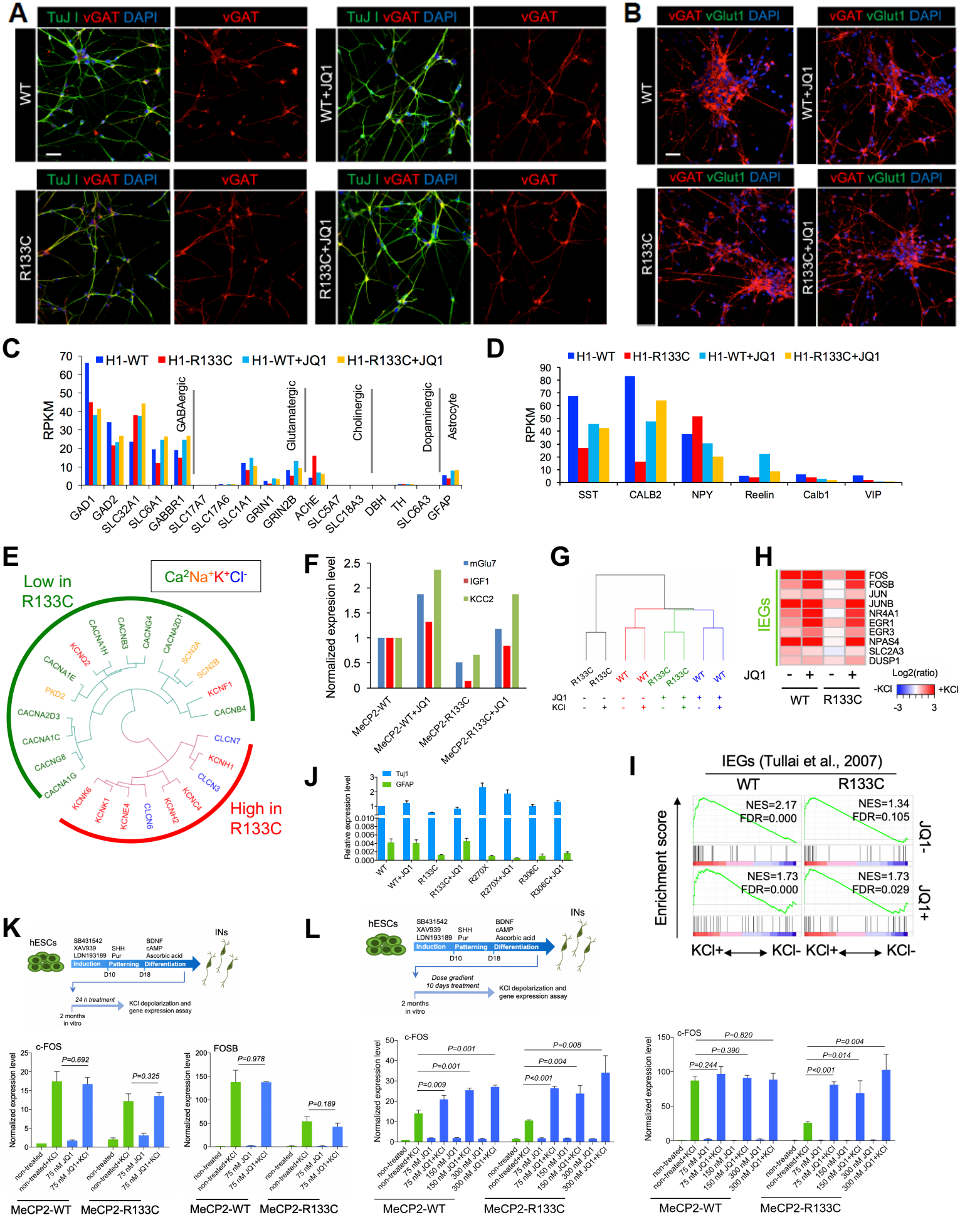
A
TuJ I vGAT DAPI
vGAT
WT
WT+JQ1
R133C
R133C+JQ1
B
vGAT vGlut1 DAPI
C
H1-WT
H1-R133C
H1-WT+JQ1
H1-R133C+JQ1
RPKM
GABAergic
Glutamatergic
Cholinergic
Dopaminergic
Astrocyte
GAD1
GAD2
SLC32A1
SLC6A1
GABBR1
SLC17A7
SLC17A6
SLC1A1
GRIN1
GRIN2B
AChE
SLC5A7
SLC18A3
DBH
TH
SLC6A3
GFAP
D
SST
CALB2
NPY
Reelin
Calb1
VIP
E
Low in R133C
Ca2Na+K+Cl-
High in R133C
F
Normalized expresion level
mGlu7
IGF1
KCC2
MeCP2-WT
MeCP2-WT+JQ1
MeCP2-R133C
MeCP2-R133C+JQ1
G
JQ1
KCl
H
IEGs
FOS
FOSB
JUN
JUNB
NR4A1
EGR1
EGR3
NPAS4
SLC2A3
DUSP1
Log2(ratio)
-KCl
+KCl
I
IEGs (Tullai et al., 2007)
Enrichment score
NES=2.17
FDR=0.000
NES=1.34
FDR=0.105
NES=1.73
FDR=0.000
NES=1.73
FDR=0.029
JQ1-
JQ1+
KCl+ KCl- KCl+ KCl-
J
Tuj1
GFAP
Relative expression level
WT
WT+JQ1
R133C
R133C+JQ1
R270X
R270X+JQ1
R306C
R306C+JQ1
K
hESCs
SB431542
XAV939
LDN193189
SHH
Pur
BDNF
cAMP
Ascorbic acid
Induction
Patterning
Differentiation
D10
D18
INs
24 h treatment
KCl depolarization and gene expression assay
2 months in vitro
L
Dose gradient 10 days treatment
c-FOS
FOSB
Normalized expression level
P=0.692
P=0.325
P=0.978
P=0.189
P=0.001
P=0.009
P=0.008
P=0.004
P<0.001
P=0.820
P=0.390
P=0.244
P=0.014
non-treated
non-treated+KCl
75 nM JQ1
75 nM JQ1+KCl
150 nM JQ1
150 nM JQ1+KCl
300 nM JQ1
300 nM JQ1+KCl
MeCP2-WT
MeCP2-R133C

Figure S4. Related with Figure 2. JQ1 Reverses the Abnormal Development of RTT INs

(A and B) Immunostaining for GABAergic marker vGAT and glutamatergic marker vGlut1 in JQ1-treated and non-treated INs. INs were treated with 75 nM JQ1 beginning at day 32, and samples were re-plated at day 65, cultured and fixed for staining at day 77. The scale bar represents 25 μm.

(C and D) Expressions of markers for various neuronal types and IN subtypes in JQ1-treated and non-treated INs. INs were treated with 75 nM JQ1 beginning at day 32, and samples were collected for RNA-seq at day 74.

(E) Dysregulation of ion channel genes in MeCP2-R133C INs (day 74).

(F) JQ1 rescued the deficient expressions of $mGlu_7$, IGF1, and KCC2 in MeCP2-R133C INs. INs were treated with 75 nM JQ1 beginning at day 32, and samples were collected for RNA-seq at day 74. RPKMs of $mGlu_7$, IGF1, and KCC2 in MeCP2-WT+JQ1, MeCP2-R133C, and MeCP2-R133C+JQ1 groups were normalized to those of MeCP2-WT INs.

(G) Hierarchical clustering of IN transcriptomes with or without JQ1 treatment. INs were treated with 75 nM JQ1 beginning at day 32, and samples were collected for RNA-seq at day 74.

(H) JQ1 rescues deficient IEG inductions in MeCP2-R133C INs under KCl depolarization. INs were treated with 75 nM JQ1 beginning at day 32, and samples were depolarized with 55 mM KCl for 1 hour, and collected for RNA-seq at day 74.

(I) GSEA analysis of depolarization-dependent IEG inductions in MeCP2-WT and MeCP2-R133C INs (day 74). Note MeCP2-R133C INs only displayed significant activity-induced IEG induction after JQ1 (75 nM) treatment.

(J) Expressions of neuronal marker Tuj1 and astrocyte marker GFAP in different MeCP2 mutant lines with or without JQ1 treatment. Mean ± SD is shown (n=3 technical repeats of the same batch of RNA pellets).

(K) IEG inductions in MeCP2-WT and MeCP2-R133C INs with acute JQ1 treatment. Day 65 INs were treated with 75 nM JQ1 for 24 hours then depolarized with 55 mM KCl for 1 hour. Mean ± SD is shown (n=3).

(L) IEG inductions in MeCP2-WT and MeCP2-R133C INs treated with different dosage of JQ1. Day 61 INs were treated with 75 nM, 150 nM, or 300 nM JQ1 for 10 days then depolarized with 55 mM KCl for 1 hour. Mean ± SD is shown (n=3).

Figure S5

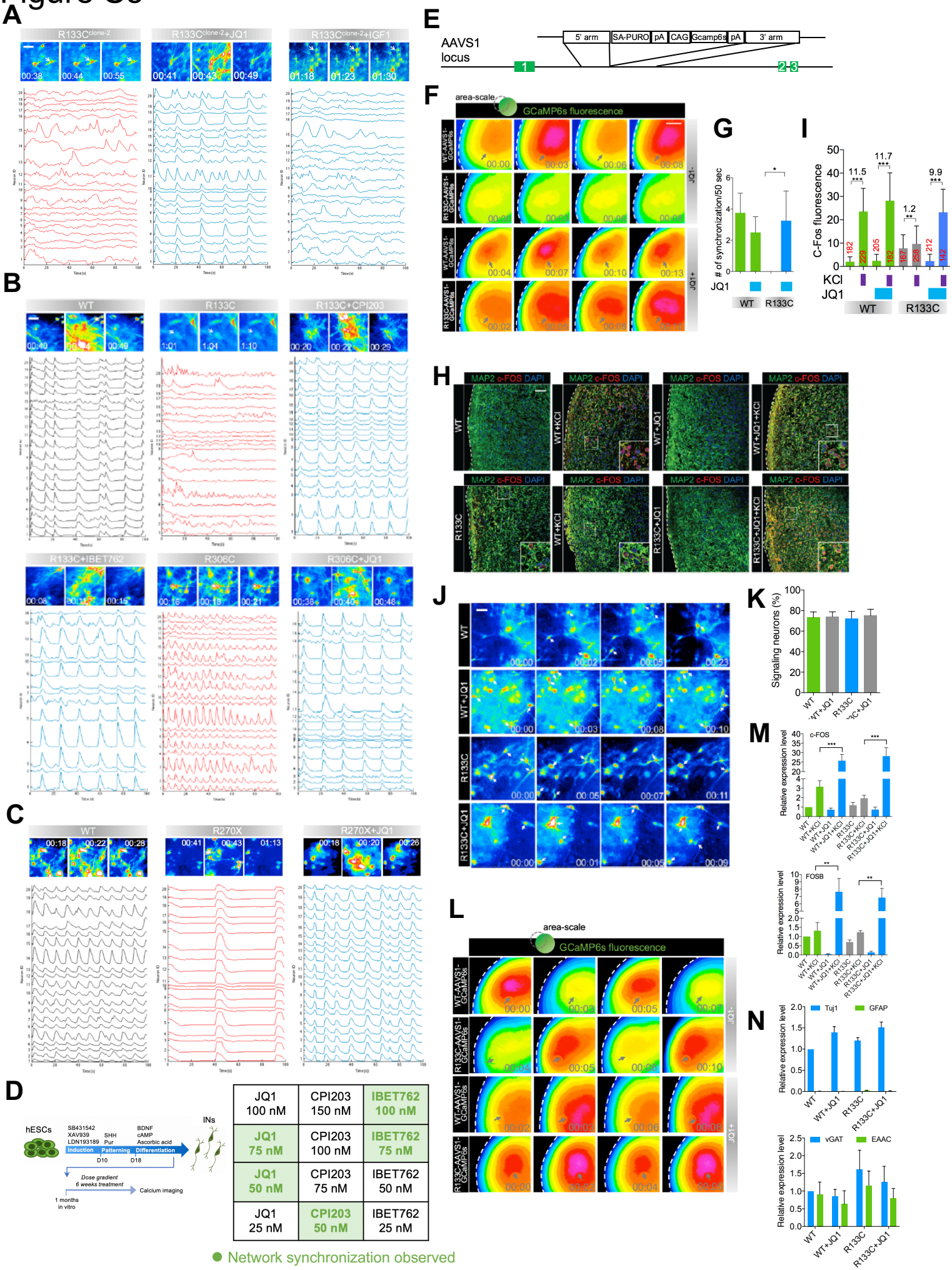
A
R133C clone-2
R133C clone-2+JQ1
R133C clone-2+IGF1
B
WT
R133C
R133C+CPI203
R133C+IBET762
R306C
R306C+JQ1
C
WT
R270X
R270X+JQ1
D
hESCs
SB431542
XAV939
LDN193189
SHH
Pur
BDNF
cAMP
Ascorbic acid
Induction
Patterning
Differentiation
D10
D18
INs
Dose gradient
6 weeks treatment
Calcium imaging
1 months
in vitro
JQ1 100 nM
CPI203 150 nM
IBET762 100 nM
JQ1 75 nM
CPI203 100 nM
IBET762 75 nM
JQ1 50 nM
CPI203 75 nM
IBET762 50 nM
JQ1 25 nM
CPI203 50 nM
IBET762 25 nM
Network synchronization observed
E
AAVS1 locus
5' arm
SA-PURO
pA
CAG
Gcamp6s
pA
3' arm
1
2-3
F
area-scale
GCaMP6s fluorescence
WT-AAVS1-GCaMP6s
R133C-AAVS1-GCaMP6s
JQ1-
JQ1+
G
# of synchronization/50 sec
JQ1
WT
R133C
I
C-Fos fluorescence
KCl
JQ1
WT
R133C
H
MAP2 c-FOS DAPI
WT
WT+KCl
WT+JQ1
WT+JQ1+KCl
R133C
R133C+KCl
R133C+JQ1
R133C+JQ1+KCl
J
WT
WT+JQ1
R133C
R133C+JQ1
K
Signaling neurons (%)
M
c-FOS
FOSB
Relative expression level
N
Tuj1
GFAP
vGAT
EAAC
Relative expression level

Figure S5. Related with Figure 2. JQ1 and its Analogues Rescues the Activities of RTT Neurons

(A) Representative images and quantification of calcium spikes from calcium imaging of INs from another independent MeCP2-R133C clone with JQ1 or IGF1 treatment. JQ1 treatment was initiated at day 32 (2 weeks of neuronal maturation), AAV1.syn.GCaMP6s vector transduction was performed at 5 weeks of neuronal maturation, and calcium imaging was performed at 8 weeks of neuronal maturation. The scale bar represents 20 μm.

(B) Representative images and quantification of calcium spikes from calcium imaging of MeCP2-WT, MeCP2-R133C and MeCP2-R306C INs without treatment, or with JQ1, CPI203, or IBET762 treatment. JQ1 (75 nM), CPI203 (50 nM), or IBET762 (100 nM) treatment was initiated at day 32 (2 weeks of neuronal maturation), AAV1.syn.GCaMP6s vector transduction was performed at 5 weeks of neuronal maturation, and calcium imaging was performed at 8 weeks of neuronal maturation. The scale bar represents 20 μm.

(C) Representative images and quantification of calcium spikes from calcium imaging of MeCP2-WT, MeCP2-R270X INs, and MeCP2-R270X INs with JQ1 treatment. JQ1 treatment was initiated at day 32 (2 weeks of neuronal maturation), AAV1.syn.GCaMP6s vector transduction was performed at 5 weeks of neuronal maturation, and calcium imaging was performed at 8 weeks of neuronal maturation. The scale bar represents 20 μm.

(D) Summary of calcium imaging in MeCP2-R133C INs treated with different dosage of BET inhibitors. The strategy of treatment and calcium imaging was the same as depicted in Figure 2D. Network synchronizations of calcium surges were only observed in conditions labeled with green color.

(E) Construct design for knocking-in GCaMP6s into the AAVS1 site.

(F and G) Representative images (F) and quantifications (G) of area-scale calcium imaging in hMGEOs. AAVS1-CAG-GCaMP6s-expressing stable H1-MeCP2-WT or H1-MeCP2-R133C lines were used for the experiments. JQ1 (75 nM) treatment was initiated at day 25 and calcium imaging was performed at day 65. Mean ± SD is shown (n=4 independently treated hMGEOs for each condition). *$p < 0.05$ (unpaired t-test). The scale bar represents 200 μm.

(H and I) Immunostaining for c-FOS and MAP2 (H) and quantifications (I) of corrected total nuclei fluorescence for c-FOS in hMGEOs, with or without KCl depolarization. JQ1 (75 nM) treatment was initiated at day 25, and at day 70 hMGEOs were depolarized with 55 mM KCl for 1 hour and processed for immunostaining and quantification. Fold changes are labeled in black. Mean ± SD is shown (n=3 independently treated hMGEOs for each condition). Cell numbers for each group are labeled in red. ***$p < 0.001$, **$p < 0.01$ (unpaired t-test). The scale bar represents 50 μm.

(J and K) Representative images from calcium imaging of MeCP2-WT and MeCP2-R133C cortical neurons with or without JQ1 treatment (J) and corresponding quantifications (K). Cortical neurons were treated with JQ1 (75 nM) beginning at day 32 (2 weeks of neuronal maturation), AAV1.syn.GCaMP6s vector transduction was performed at 5 weeks of neuronal maturation, and calcium imaging was performed at 8 weeks of neuronal maturation. Quantifications of signaling neurons are shown on the right. Mean ± SD is shown (n=4 independently treated wells). The scale bar represents 25 μm.

(L) Representative images of area-scale calcium imaging of MeCP2-WT and MeCP2-R133C hCOs with or without JQ1 treatment. AAVS1-CAG-GCaMP6s-expressing stable H1-MeCP2-WT or H1-MeCP2-R133C lines were used for the experiments. JQ1 (75 nM) treatment was initiated beginning at day 25 and calcium imaging was performed at day 65. The scale bar represents 200 μm.

(M) Inductions of c-FOS and FOSB in MeCP2-WT and MeCP2-R133C cortical neurons by KCl depolarization, with or without JQ1 treatment, detected by qPCR. Cortical neurons were treated with JQ1 (75 nM) beginning at day 32 (2 weeks of neuronal maturation), and at day 75 samples were depolarized with 55 mM KCl for 1 hour and processed for qPCR. Mean ± SD is shown (n=3 technical repeats of the same batch of RNA pellets). ***$p < 0.001$, **$p < 0.01$ (unpaired t-test).
(N) Expressions of neuronal marker Tuj1, astrocyte marker GFAP, GABAergic marker vGAT, and glutamatergic marker EAAC in MeCP2-WT and MeCP2-R133C cortical neurons with or without JQ1 treatment, detected by qPCR. Cortical neurons were treated with JQ1 (75 nM) beginning at day 32 (2 weeks of neuronal maturation), and at day 75 samples were depolarized with 55 mM KCl for 1 hour and processed for qPCR. Mean ± SD is shown (n=3 technical repeats of the same batch of RNA pellets).

Figure S6

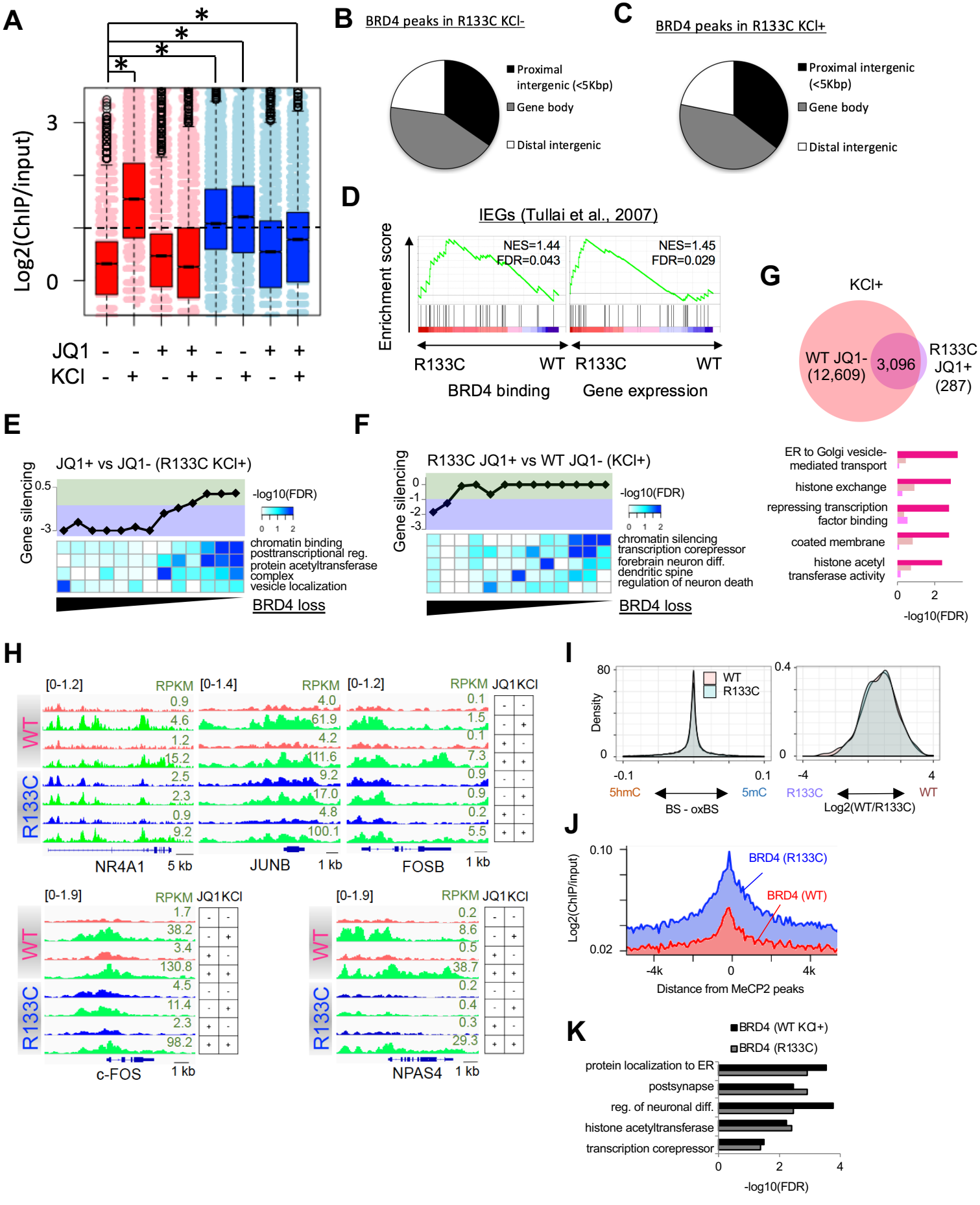
A
Log2(ChIP/input)
JQ1
KCl
B
BRD4 peaks in R133C KCl-
Proximal intergenic (<5Kbp)
Gene body
Distal intergenic
C
BRD4 peaks in R133C KCl+
Proximal intergenic (<5Kbp)
Gene body
Distal intergenic
D
IEGs (Tullai et al., 2007)
Enrichment score
NES=1.44 FDR=0.043
NES=1.45 FDR=0.029
R133C
WT
BRD4 binding
Gene expression
G
KCl+
WT JQ1- (12,609)
3,096
R133C JQ1+ (287)
E
JQ1+ vs JQ1- (R133C KCl+)
Gene silencing
-log10(FDR)
chromatin binding
posttranscriptional reg.
protein acetyltransferase complex
vesicle localization
BRD4 loss
F
R133C JQ1+ vs WT JQ1- (KCl+)
Gene silencing
-log10(FDR)
chromatin silencing
transcription corepressor
forebrain neuron diff.
dendritic spine
regulation of neuron death
BRD4 loss
ER to Golgi vesicle-mediated transport
histone exchange
repressing transcription factor binding
coated membrane
histone acetyl transferase activity
-log10(FDR)
H
WT
R133C
RPKM
JQ1 KCl
NR4A1
JUNB
FOSB
c-FOS
NPAS4
5 kb
1 kb
I
WT
R133C
Density
5hmC
5mC
BS - oxBS
R133C
WT
Log2(WT/R133C)
J
BRD4 (R133C)
BRD4 (WT)
Log2(ChIP/input)
Distance from MeCP2 peaks
K
BRD4 (WT KCl+)
BRD4 (R133C)
protein localization to ER
postsynapse
reg. of neuronal diff.
histone acetyltransferase
transcription corepressor
-log10(FDR)

Figure S6. Related with Figure 3 and Figure 4. BRD4 Mediates the Abnormal Transcriptions in MeCP2-R133C INs

(A) Comparative analysis of BRD4 binding intensity under JQ1 and KCl treatment. * represents $p<0.05$ by two-side T test.

(B and C) Distributions of BRD4 binding site in MeCP2-R133C INs before or after KCl depolarization.

(D) GSEA for putative IEGs between MeCP2-WT and MeCP2-R133C INs. Genes are sorted by BRD4 binding intensity (left) or expression difference (right).

(E) Silencing of gene transcription by loss of chromatin BRD4 compared between JQ1-treated, KCL-depolarized MeCP2-R133C INs and non-treated, KCl-depolarized MeCP2-R133C INs. BRD4 peaks are sorted by log2(JQ1+/JQ1-) in MeCP2-R133C INs with KCl depolarization.

(F) Silencing of gene transcription by loss of chromatin BRD4 compared between JQ1-treated, KCl-depolarized MeCP2-R133C INs and non-treated, KCl-depolarized MeCP2-WT INs. BRD4 peaks are sorted by log2((MeCP2-R133C JQ1+)/(MeCP2-WT)) with KCl depolarization.

(G) Comparison of BRD4 chromatin binding sites between non-treated, KCl-depolarized MeCP2-WT INs and JQ1-treated, KCl-depolarized MeCP2-R133C INs (upper panel). GOs of genes that showed an activity-dependent BRD4 recruitment in non-treated, KCl-depolarized MeCP2-WT INs and JQ1-treated, KCl-depolarized MeCP2-R133C INs are shown in the bottom panel. Bar colors in the bottom panel correspond to Venn diagram colors in upper panel.

(H) BRD4 binding tracks in IEGs and the corresponding transcription levels in MeCP2-WT and MeCP2-R133C INs with or without JQ1 treatment, depolarized or non-depolarized with KCl. Note that gene showed either increased (NR4A1, JUNB, FOSB, and c-FOS) or normal (NPAS4) BRD4 recruitment in MeCP2-R133C INs at basal level, but only gained depolarization-induced BRD4 recruitment after JQ1 treatment. Corresponding RPKM from RNA-seq data is labeled in green.

(I) Difference of 5hmC level on CpGIs (left) and MeCP2 binding to 5hmC-enriched CpGIs (right) between MeCP2 WT and MeCP2-R133C.

(J) Co-localization of WT MeCP2 peaks with BRD4 peaks in MeCP2-R133C INs and depolarized MeCP2-WT INs.

(K) Significant GO terms for common target genes shown in Figure 4C.

Figure S7

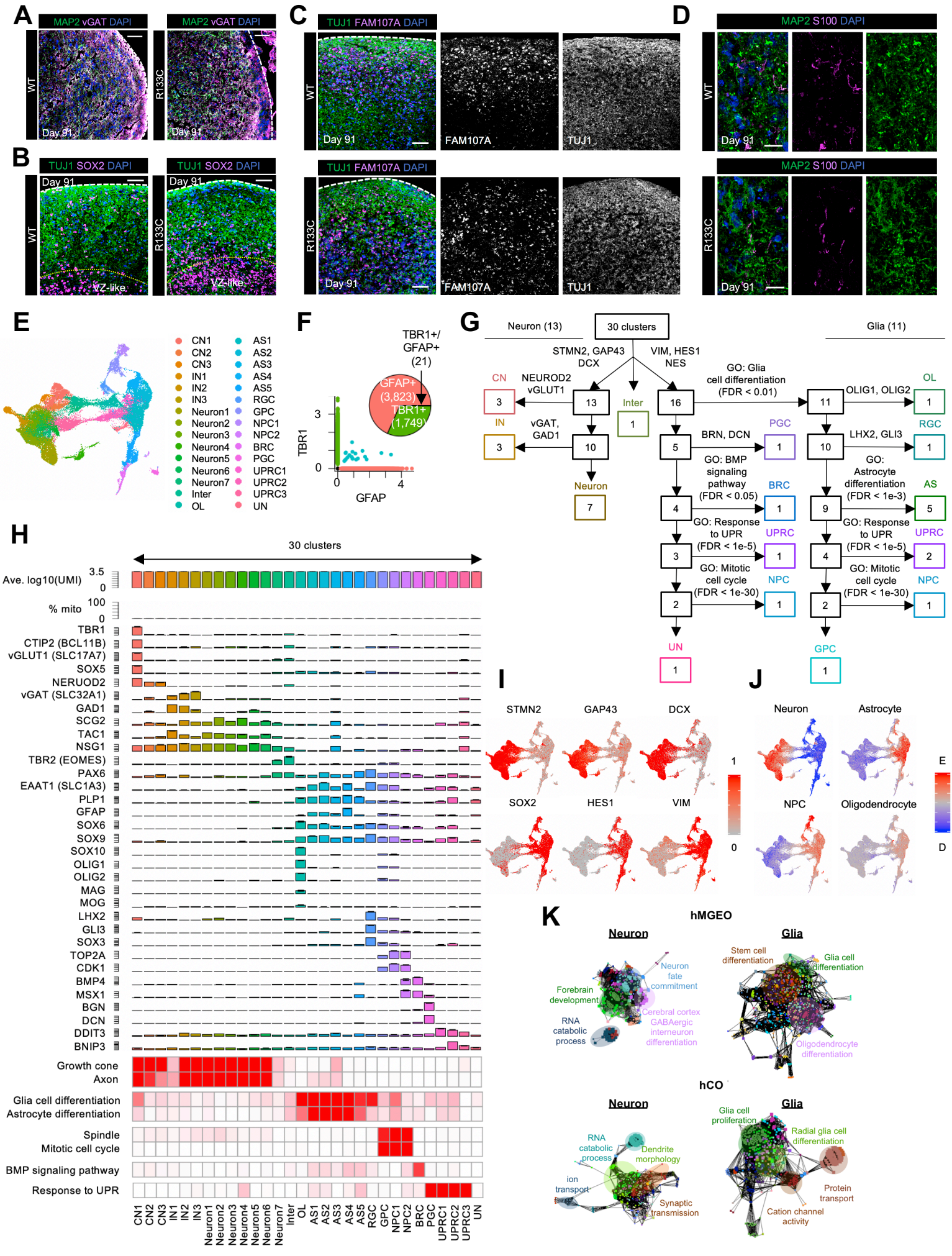
A
MAP2 vGAT DAPI
WT
R133C
Day 91
B
TUJ1 SOX2 DAPI
VZ-like
C
TUJ1 FAM107A DAPI
FAM107A
TUJ1
D
MAP2 S100 DAPI
E
CN1
CN2
CN3
IN1
IN2
IN3
Neuron1
Neuron2
Neuron3
Neuron4
Neuron5
Neuron6
Neuron7
Inter
OL
AS1
AS2
AS3
AS4
AS5
RGC
GPC
NPC1
NPC2
BRC
PGC
UPRC1
UPRC2
UPRC3
UN
F
TBR1+/
GFAP+
(21)
GFAP+
(3,823)
TBR1+
(1,749)
TBR1
GFAP
G
Neuron (13)
30 clusters
Glia (11)
STMN2, GAP43
DCX
VIM, HES1
NES
CN
NEUROD2
vGLUT1
IN
vGAT,
GAD1
Neuron
Inter
GO: Glia
cell differentiation
(FDR < 0.01)
OLIG1, OLIG2
OL
RGC
BRN, DCN
PGC
LHX2, GLI3
GO: BMP
signaling
pathway
(FDR < 0.05)
BRC
GO:
Astrocyte
differentiation
(FDR < 1e-3)
AS
GO: Response
to UPR
(FDR < 1e-5)
UPRC
GO: Mitotic
cell cycle
(FDR < 1e-30)
NPC
UN
GPC
H
30 clusters
Ave. log10(UMI)
% mito
TBR1
CTIP2 (BCL11B)
vGLUT1 (SLC17A7)
SOX5
NERUOD2
vGAT (SLC32A1)
GAD1
SCG2
TAC1
NSG1
TBR2 (EOMES)
PAX6
EAAT1 (SLC1A3)
PLP1
GFAP
SOX6
SOX9
SOX10
OLIG1
OLIG2
MAG
MOG
LHX2
GLI3
SOX3
TOP2A
CDK1
BMP4
MSX1
BGN
DCN
DDIT3
BNIP3
Growth cone
Axon
Glia cell differentiation
Astrocyte differentiation
Spindle
Mitotic cell cycle
BMP signaling pathway
Response to UPR
I
STMN2
GAP43
DCX
SOX2
HES1
VIM
J
Neuron
Astrocyte
NPC
Oligodendrocyte
K
hMGEO
Neuron
Glia
Forebrain development
Neuron fate commitment
RNA catabolic process
Cerebral cortex GABAergic interneuron differentiation
Stem cell differentiation
Glia cell differentiation
Oligodendrocyte differentiation
hCO
Glia cell proliferation
Radial glia cell differentiation
Dendrite morphology
ion transport
Synaptic transmission
Protein transport
Cation channel activity

Figure S7. Related with Figure 6. Effects of JQ1 on Regionally Specified Human Brain Organoids

(A) Immunostaining for MAP2 and vGAT in hMGEOs. The scale bar represents 50 μm.

(B) Immunostaining for TUJ1 and SOX2 in hCOs. The scale bar represents 50 μm.

(C and D) Immunostaining for TUJ1 and FAM107A (C), MAP2 and S100 (D) in hCOs. The scale bar represents 50 μm in C, and 12.5 μm in D.

(E) tSNE plot of single cells distinguished by clusters.

(F) Evaluation of double frequency. Log2(normalized UMI) of GFAP and TBR1 are plotted at X and Y axis, respectively.

(G) Schematic representation of cluster annotation.

(H) UMI counts, percentage of mitochondria DNAs, expression of cell type-specific genes across and enrichment of Gene Ontology across 30 clusters. Bar graphs represent Mean ± SD. Heatmaps represent –log10(FDR) of GO terms.

(I) Expression patterns of genes related with early neurogenesis and neuronal growth cone.

(J) Enrichment of gene signatures for neuron NPC, astrocyte and oligodendrocyte. Enrichment and depletion are scaled by –log10(FDR) and shown by read and blue colors, respectively.

(K) ClueGO network for genes rescued by JQ1 in hMGEOs (top) and hCOs (bottom).

See also Figure 6.